

pubs.acs.org/JPCA Article

Detailed Reaction Kinetics for Hydrocarbon Fuels: The Development and Application of the ReaxFF_{CHO}-S22 Force Field for C/H/O Systems with Enhanced Accuracy

Qingqing Wang, Qi He, Bin Xiao, Dong Zhai, Yiheng Shen, Yi Liu,* and William A. Goddard, III



Cite This: J. Phys. Chem. A 2024, 128, 5065–5076



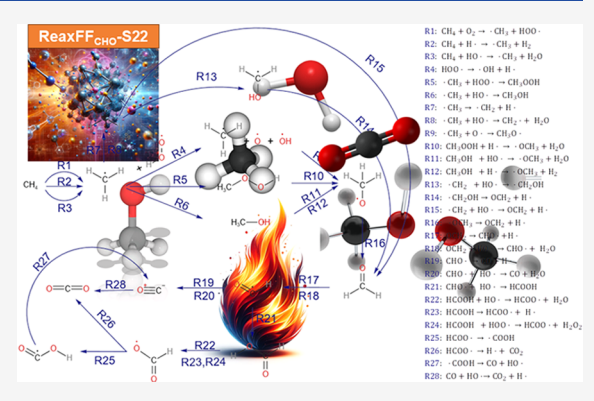
ACCESS I

Metrics & More

Article Recommendations

Supporting Information

ABSTRACT: Efficient and accurate reactive force fields (e.g., ReaxFF) are pivotal for large-scale atomistic simulations to comprehend microscopic combustion processes. ReaxFF has been extensively utilized to describe chemical reactions in condensed phases, but most existing ReaxFF models rely on quantum mechanical (QM) data nearly two decades old, particularly in hydrocarbon systems, constraining their accuracy and applicability. Addressing this gap, we introduce a reparametrized ReaxFF_{CHO}-S22 for C/H/O systems, tailored for studying the pyrolysis and combustion of hydrocarbon fuel. Our approach involves high-level QM benchmarks and large database construction for C/H/O systems, global ReaxFF parameter optimization, and molecular dynamics simulations of typical hydrocarbon fuels. Density functional theory (DFT) computations utilized the M06-2X functional at the meta-generalized



gradient approximation (meta-GGA) level with a large basis set $(6-311++G^{**})$. Our new ReaxFF_{CHO}-S22 model exhibits a minimum 10% enhancement in accuracy compared to the previous ReaxFF models for a large variety of hydrocarbon molecules. This advanced ReaxFF_{CHO}-S22 not only enables efficient large-scale studies on the microscopic chemical reactions of more complex hydrocarbon fuel but also can extend to biofuels, energetic materials, polymers, and other pertinent systems, thus serving as a valuable tool for studying chemical reaction dynamics of the large-scale hydrocarbon condensed phase at an atomistic level.

1. INTRODUCTION

The study of combustion reactions is fundamentally linked to the energy, environmental, and transportation sectors. A deep and systematic understanding of microscopic combustion mechanisms is crucial not only for comprehending the scientific principles underlying combustion phenomena but also for addressing practical challenges in these sectors, e.g., efficient energy generation and pollution reduction. Quantum mechanics (QM) has been instrumental in detailing reaction mechanisms in which the description of chemical bond formation and breakage is critical. Nonetheless, the application of QM to the study of reaction dynamics for large-scale hydrocarbon pyrolysis and combustion at high temperatures and pressures is limited by the enormous computational demands in solving self-consistently the Schrodinger equation for the electron distribution of realistic systems.

Reactive Molecular Dynamics (RMD) merges the reactive force field (ReaxFF) with Molecular Dynamics (MD) to model large-scale reactions at the molecular level. Developed originally by Goddard III, van Duin, and colleagues, ReaxFF is a classical molecular force field (FF) that uses bond order to describe the formation and rupture of chemical bonds. This capability allows for the simulation of chemical reactions without the need to predefine reaction paths, an essential feature for tackling

complex chemical reaction problems. The Electronegativity Equalization Method (EEM) 7 or Charge Equilibration Method (QEq) 8 is utilized within this framework to adjust dynamically charge distribution depending on configurations, enabling the explicit inclusion of electrostatic interactions. ReaxFF Molecular Dynamics can simulate the dynamics of systems efficiently from several thousands to million atoms, offering a significant scale-up in length and time scales compared with expensive QM dynamics.

The ReaxFF reactive force field has seen a remarkable expansion in its application scope over recent years, touching various corners of material science, chemistry, and physics. This broad applicability stems from its unique ability to accurately model the formation and dissociation of chemical bonds in a dynamic and reactive environment. ReaxFF has influenced research across various fields including hydrocarbon fuel, 9-17 energetic materials, 18-24 propellants, 25 polymer, 26-35 metals, 36

Received: March 23, 2024 Revised: May 28, 2024 Accepted: June 3, 2024 Published: June 13, 2024





and oxides,^{37,38} with the special effectiveness in studying the combustion and pyrolysis of hydrocarbon fuels.^{9,17}

The microscopic mechanisms underlying the high-temperature pyrolysis and combustion of hydrocarbon fuels represent a complex challenge due to the multitude of instantaneous reactions and intermediates involved simultaneously. ReaxFF's capability to efficiently describe these complex reaction networks makes it particularly suited for such studies. ^{10,33} It allows for an atomistic simulation of the entire combustion process, from the initial reactants through various intermediate species to the final combustion products. This includes the ability to describe transient species and detailed reaction pathways that are difficult to observe experimentally.

The development and refinement of ReaxFF are closely tied to the availability of a reliable quantum mechanics (QM) data set and an effective algorithm for parameter optimization. Historically, the QM data set underpinning most ReaxFF models used the B3LYP hybrid functional of density functional theory with a 6-31G* basis set, which has been constructed nearly two decades ago.³⁹ Additionally, the Mulliken charge model, commonly used for determining atomic charges in the QM data set, has been criticized for its dependency on the basis set, potentially misrepresenting charge transfer dynamics.

To address these issues, this work introduces a new generation ReaxFF, designated ReaxFF $_{\text{CHO}}$ -S22, for carbon, hydrogen, and oxygen (C/H/O) systems, based on a meta-generalized gradient approximation (meta-GGA) level QM data set. This data set includes various equilibrium molecular configurations and their derivatives generated using the M06-2X functional combined with a large 6-311++G** basis set. We employ the ADCH charge model for more accurate and robust atomic charge calculations and utilize a genetic algorithm (GA) for the global optimization of ReaxFF parameters, aiming to overcome the limitations of local optimization methods.

Employing the ReaxFF_{CHO}-S22, molecular dynamics simulations were performed on several key processes such as methane pyrolysis, methane oxidation, and *n*-dodecane pyrolysis to illustrate the power of the new description. The outcomes of these simulations validate the force field's capability to accurately model the dynamic behavior of hydrocarbons under various conditions.

This paper is structured as follows: Section 2 outlines the theoretical methods and computational details; Section 3 discusses the development of the new ReaxFF for C/H/O systems alongside computational results of pyrolysis and combustion of hydrocarbon fuels; and Section 4 concludes with a summary of our findings. Detailed raw data and new force field parameters are provided in the Supporting Information.

2. COMPUTATIONAL METHODS

2.1. ReaxFF Force Field Method. The ReaxFF force field, a type of classical empirical force field, sets itself apart from traditional nonreactive force fields through its use of the bond order (BO) formalism to describe bond formation, dissolution, and rearrangements. This approach allows for dynamic assessment of atomic connectivity, interpreting changes in bond order as the formation or breakage of bonds during reactive molecular dynamics. The total energy of a system under ReaxFF is calculated as a sum of various energy components, each representing a different type of physical interaction within the molecule: ⁶

$$\begin{split} E_{\rm system} &= E_{\rm bond} + E_{\rm lp} + E_{\rm over} + E_{\rm under} + E_{\rm val} + E_{\rm pen} \\ &\quad + E_{\rm coa} + E_{\rm C2} + E_{\rm tors} + E_{\rm conj} + E_{\rm Hbond} + E_{\rm vdW} \\ &\quad + E_{\rm Coulomb} \end{split} \tag{1}$$

These terms account for bond energy, lone-pair energy, penalties for over- and undercoordination, valence-angle energy, penalties for bond configuration issues, conjugation and torsion energies, hydrogen bond energy, van der Waals forces, and Coulombic interactions, respectively. Initially developed for hydrocarbons (elements C and H) by Goddard III and van Duin et al., 6 the ReaxFF force field was later extended to include oxygen parameters for combustion studies. 9 Further developments by Ashraf and van Duin expanded its application to the combustion of small hydrocarbons and CO₂ to CO conversion. 16

2.2. Quantum Mechanical Calculations. In this study, the development and validation of new ReaxFF parameters for C/ H/O hydrocarbons were underpinned by a comprehensive QM database, meticulously constructed by using density functional theory (DFT). The foundation of our computational approach was laid by employing the Gaussian 09 software suite, 43 a choice that ensured the reliability and accuracy of our QM calculations. The M06-2X density functional, renowned for its effectiveness in capturing the intricacies of thermochemistry, noncovalent interactions, and transition states, was selected for this purpose. 44 Complementing this, the large 6-311++G** Popletype basis set was utilized, offering extensive and precise electron distribution calculations. Our computations also incorporated spin polarization, a critical factor in accurately modeling systems with unpaired electrons, thereby enhancing the fidelity of our simulations.

The QM database crafted for this work encompasses a wide array of data crucial for the accurate parametrization of the ReaxFF force field. This includes detailed geometry and potential energy results such as bond dissociation energy curves, which are pivotal for understanding the strength and stability of chemical bonds for a variety of geometries. Distortion energy curves as a function of bond, angle, and torsion angle were generated to provide valuable insights into the energy variations associated with varied valence bonds, valence angles, and torsional angles, respectively. Moreover, key reaction energies were meticulously evaluated by using the newly developed ReaxFF parameters, ensuring reasonable thermodynamics of chemical reactions involved in pyrolysis and combustion.

For researchers and practitioners seeking deeper insights and additional data, the Supporting Information section serves as a valuable resource. It offers extended details and results, facilitating a comprehensive understanding of the QM database and the underpinning calculations that have significantly contributed to the advancement of the ReaxFF parametrization for C/H/O hydrocarbons.

2.3. Molecular Dynamics Simulations. Additional validations of the new ReaxFF parameters for C/H/O systems were assessed through a series of MD simulations of pyrolysis and combustion processes for hydrocarbon fuels. These simulations were executed utilizing the reax/c package within the Large-scale Atomic/Molecular Massively Parallel Simulator (LAMMPS) software, a product of collaborative efforts with Sandia National Laboratories. 45,46 This computational tool is renowned for its robustness and versatility in handling reactive force field simulations across a wide range of chemical systems.

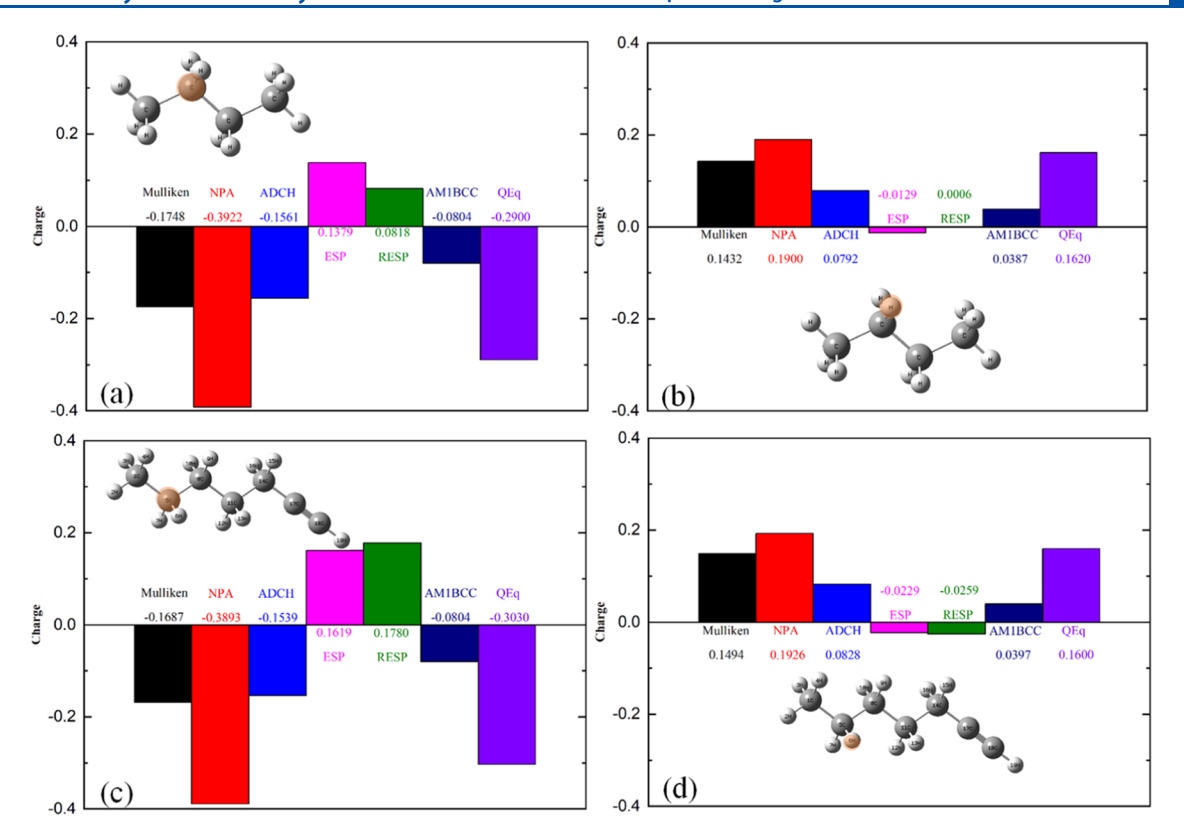


Figure 1. Charge comparison among Mulliken, NPA, ADCH, ESP, RESP, AM1-BCC, and Qeq schemes for (a) the C and (b) the H ions (in yellow) of *n*-butane and (c) the C and (d) the H ions (in yellow) of n-heptyne.

Utilizing the new force field parameters, we embarked on a series of MD simulations involving various hydrocarbon fuels. These simulations were designed to probe the behavior of these fuels under a spectrum of conditions, including variations in the temperature, density, and oxygen equivalent ratio. By systematically altering these conditions, we were able to observe and document the reactivity and stability of hydrocarbon fuels, providing a comprehensive picture of pyrolysis and combustion behaviors in different environmental contexts.

The comprehensive analysis of the simulation outcomes was performed using the Visualization and Analysis of ReaxFF Molecular Dynamics (VARxMD) tool, a sophisticated analysis framework developed by Li's research group. ^{47–49} This tool, designed specifically for ReaxFF simulations, enables a detailed examination of reaction dynamics, providing insights into the behavior of chemical species throughout the simulation process. Additionally, our research team employed custom in-house code to further dissect and understand the nuances of the simulation data, allowing for a tailored analysis that addressed the specific objectives of our study. Section 3.2 delves deeper into the specifics of these simulations, offering detailed insights into the methodologies employed, the conditions tested, and the key findings obtained from these investigative efforts.

3. RESULTS AND DISCUSSION

3.1. Construction of QM database for Hydrocarbon Molecules. The construction of a QM database for force field (FF) development involves a comprehensive approach that addresses several critical aspects to ensure that the database is versatile and effective for simulating molecular behaviors. Here are the key considerations involved in constructing such a QM database:

Table 1. Comparison of Shielding γ (EEM type), Electronegativity η , and Hardness η Charge Parameters for C/H/O Elements in Various ReaxFF_{CHO}

charge parameters	ReaxFF _{CHO} 08	ReaxFF _{CHO} 16	ReaxFF _{CHO} -S22
γ_{C}	0.9000	0.9500	0.8148
χ_{C}	5.8678	5.0191	5.7420
$\eta_{ m C}$	7.0000	7.0500	7.4185
$\gamma_{ m H}$	1.0206	0.9900	0.6930
$\chi_{ m H}$	5.3200	4.7757	3.8849
$\eta_{ m H}$	7.4366	9.7732	8.2954
γο	1.0503	0.9900	1.2870
χο	8.5000	7.9703	7.6358
$\eta_{ m O}$	8.9989	7.0500	8.1402
⟨RMSE⟩	0.03	0.05	0.02

- (1) Geometries of Molecules: The database must contain detailed information on the geometries of molecules in various states. This includes equilibrium geometries where the molecules are in their most stable form, as well as nonequilibrium geometries that represent transitional states, reactant, or product states in chemical reactions or molecules under external stress. Capturing a wide range of geometries is crucial for developing FFs that can accurately predict molecular structures and behaviors under different conditions.
- (2) Energies of Molecules: Alongside geometrical data, the database should include energy information for the molecules in their different geometrical states. This includes ground state energies, excited state energies, and the energy changes associated with transitions between different states. Accurate energy data is essential for FFs to correctly predict the dynamics of molecules,

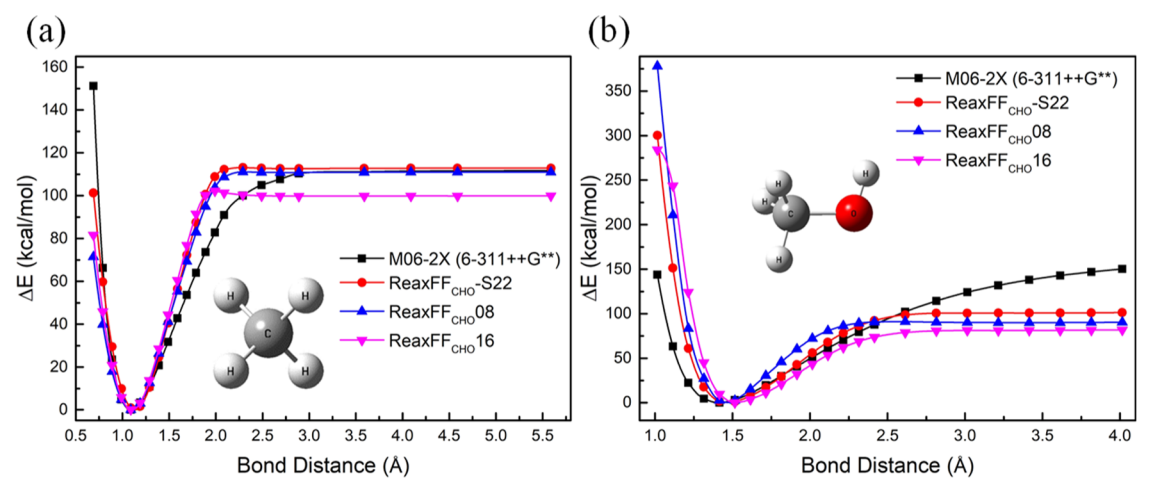


Figure 2. Valence bond dissociation energy as functions of distance described by various ReaxFF_{CHO} vs QM (DFT/M06-2X/6-311++G**): (a) the C-H bond in methane and (b) the C-O bond in methanol. Red, gray, and white spheres represent O, C, and H atoms, respectively.

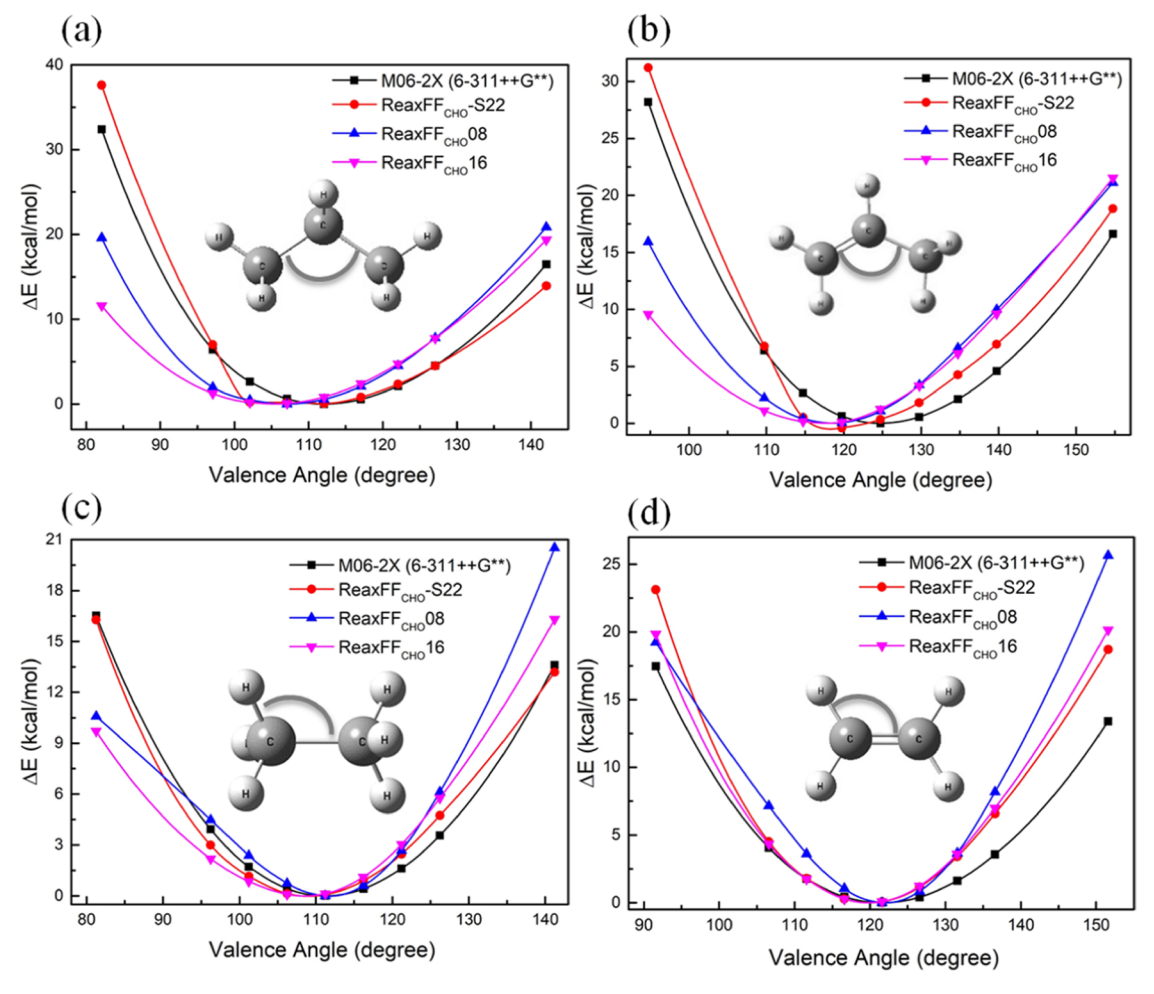


Figure 3. Valence-angle distortion energy as functions of angle described by various ReaxFF $_{CHO}$ vs QM (DFT/M06-2X/6-311++G**): (a) the C-C-C angle, (b) the C=C-C angle, (c) the C-C-H angle, and (d) the C=C-H angle. Gray and white spheres represent C and H atoms, respectively.

including reaction kinetics, stability, and interactions with other molecules.

(3) Scalability to Various Molecule Sizes: The database should cover a wide range of molecule sizes, from small molecules to large hydrocarbon molecules. This scalability is vital because the complexity of molecular interactions and the types of forces that become significant can change with the size of the molecule. For instance, while van der Waals forces play crucial roles in large hydrocarbon molecules, covalent bonding and ionic interactions might be more relevant for small molecules.

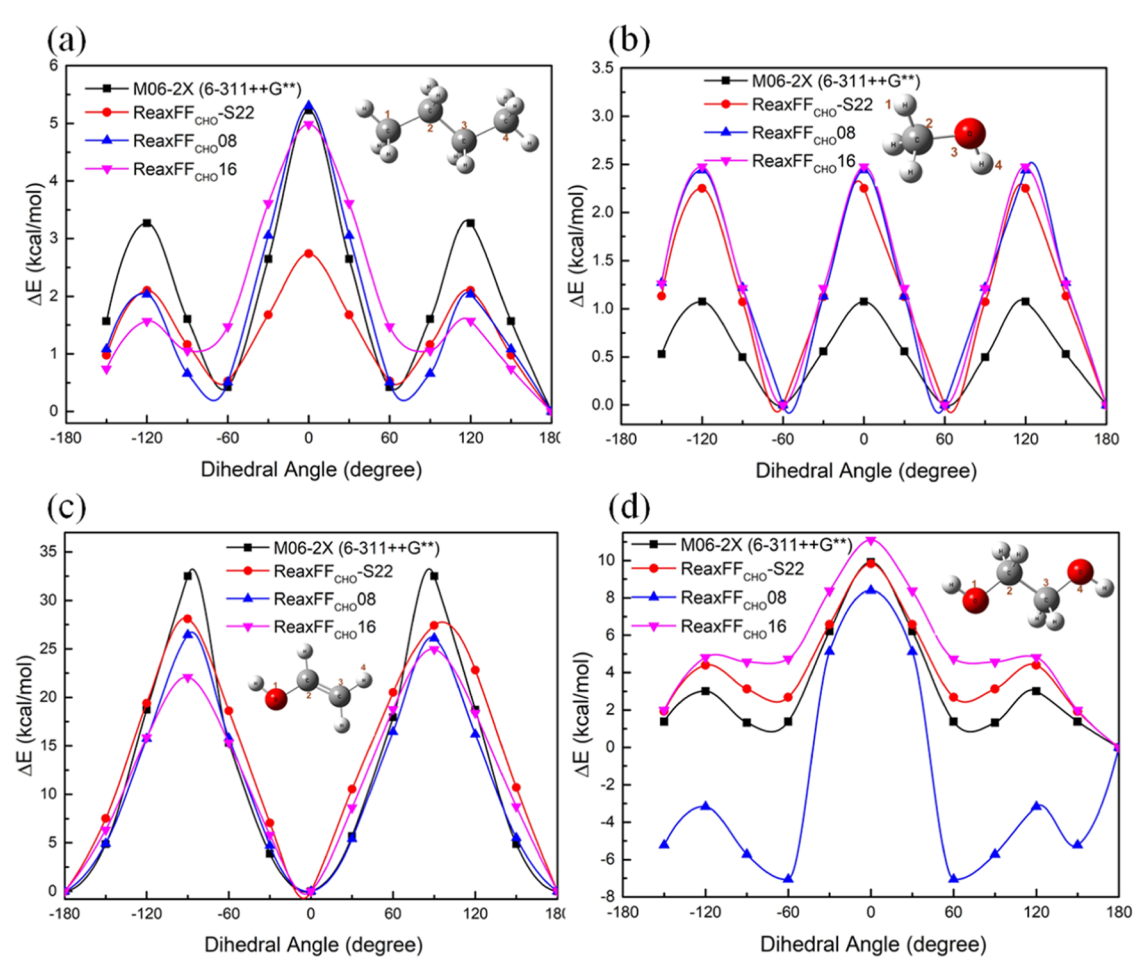


Figure 4. Torsion angle distortion energy as functions of torsion angle described by various ReaxFF $_{CHO}$ vs QM (DFT/M06-2X/6-311++G**): (a) the C-C-C-C torsion angle, (b) the H-C-O-H torsion angle, (c) the O-C=C-H torsion angle, and (d) the O-C-C-O torsion angle. Red, gray, and white spheres represent O, C, and H atoms, respectively.

Table 2. Averaged $\langle RMSE \rangle$ (in kcal/mol) for the Energy Testing Sets of Hydrocarbon Molecules Grouped by the Number of Carbon Atoms Described by Various ReaxFF_{CHO}

⟨RMSE⟩ (kcal/mol)	C_5	C_6	C ₇	C_8
ReaxFF _{CHO} -S22	10.63	11.74	9.62	12.26
ReaxFF _{CHO} 16	12.35	13.29	11.12	13.74
$ReaxFF_{CHO}08$	12.53	12.61	9.96	13.31

(4) Relevance to Various Application Scenarios: The molecules and their associated data in the database should be selected not only based on their theoretical interest but also considering their relevance to practical applications. This means including molecules that are important in combustion process. By doing so, the developed FFs can be directly applied to solve real-world combustion problems.

In this study, we aim to develop a ReaxFF capable of describing both small and large hydrocarbon molecules with applications in gasoline and diesel combustion. Therefore, we constructed a QM database containing hydrocarbon molecules with 1–8 C atoms at all possible polymorph forms including straight chains, branched chains, and cyclic molecules, plus Ocontaining molecules like $\rm H_2O$ or $\rm CO_x$ (x=1,2), etc. Specifically, the QM database consists of 27765 equilibrium and deformed molecules that can be classified according to the

number of C atoms into C0–C4 (1006), C5 (959), C6 (2077), C7 (5070), and C8 (18653), respectively. Among these categories, the small molecule group C0–C4 was used for training ReaxFF energy parameters, while the other large molecule groups were used for FF validation. It allows for the development of a force field that is grounded in fundamental interactions while being tested against more complex systems. The 27765 molecules in the whole QM data set also can be geometrically classified into equilibrium geometries (306), the flexible deformation scan of bonds (8455), angles (9458), and torsions (9470) as well as key chemical reactions (76) related to combustion.

To generate potentially key radicals from pyrolysis or combustion of typical straight and branched hydrocarbons, we employed the Reaction Mechanism Generator (RMG), an automated tool that constructs efficiently detailed chemical kinetic mechanisms from a comprehensive chemistry database. The radicals critical to our study were subsequently optimized using QM methods and added into the ReaxFF training data sets. The training set also contains a number of key reactions related to the combustion of hydrocarbon fuels (Figures S1–S3).

3.2. Optimization of ReaxFF Force Field Parameters. 3.2.1. Optimization of Charge Parameters. QM offers several definitions of atomic charges based on the different partition schemes of electron populations. In this study, we evaluated

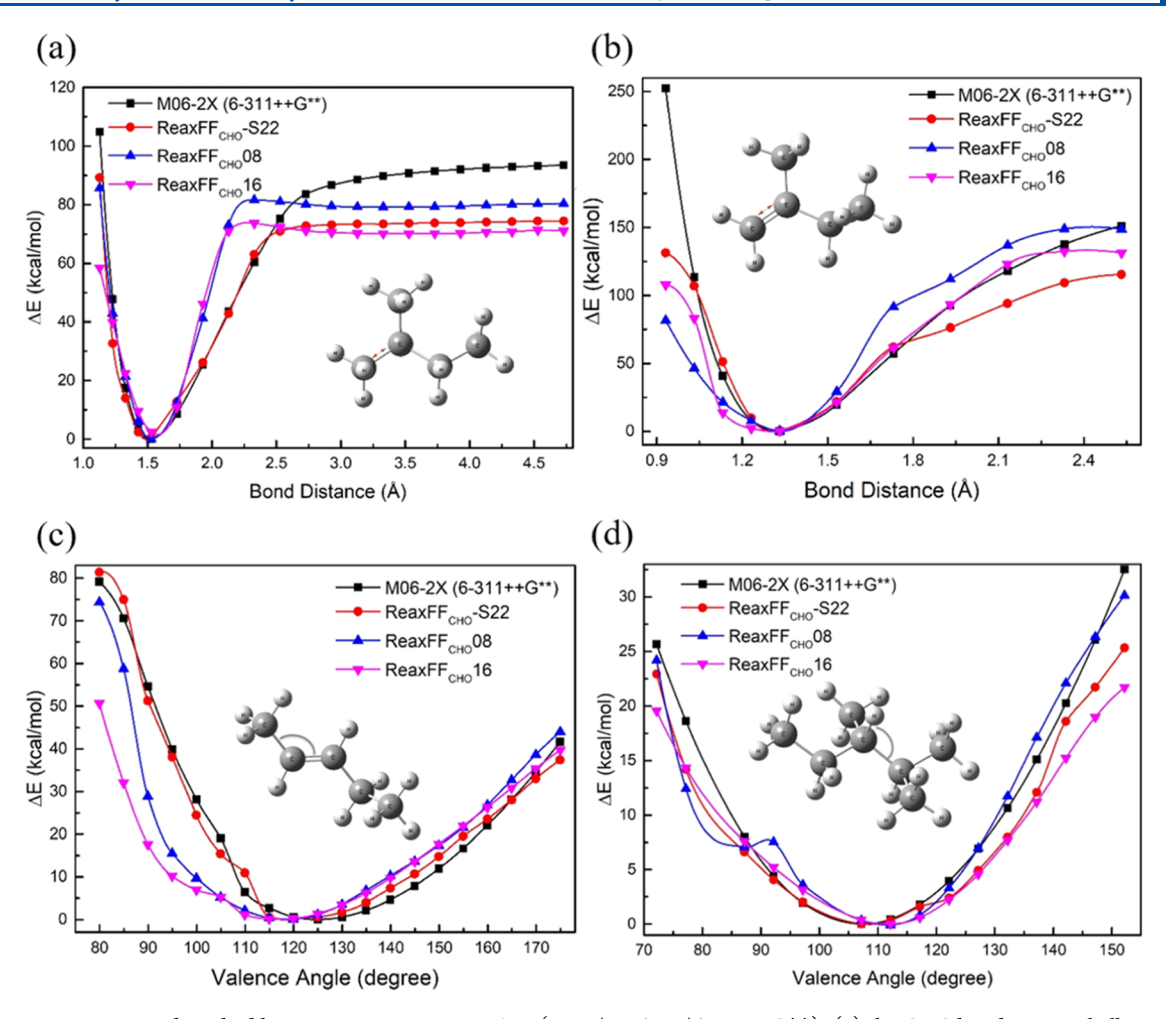


Figure 5. Distortion energy described by various ReaxFF $_{CHO}$ vs QM (DFT/M06-2X/6-311++G**): (a) the C-C bond in 2-methylbutane, (b) the C=C bond in 2-methylbutene, (c) the C-C=C angle in 2-pentene, and (d) the C-C-H angle in 2,3-dimethylpentane. Gray and white spheres represent C and H atoms, respectively.

various charge calculation methods, including Mulliken, ^{51–53} Natural Population Analysis (NPA), ⁵⁴ Average Density Derived Coulomb Hamiltonian (ADCH), ⁴¹ Electrostatic Potential (ESP), ^{55–57} Restrained Electrostatic Potential (RESP), ⁵⁸ AM1-Bond Charge Correction (AM1-BCC), ^{59,60} and Charge Equilibration (QEq), ⁸ using *n*-butane and n-heptyne molecules as examples (Figure 1). Our analysis revealed inconsistencies in the ESP and RESP charges for the C atoms, contradicting expected electronegativity trends that should lead to charge transfer from the H to C atoms. Additionally, the AM1-BCC and QEq methods tended to underestimate and overestimate the magnitudes of the atomic charges, respectively. Despite the common use of Mulliken charges in previous ReaxFF development, their suitability diminishes with larger basis sets chosen in this work for better QM accuracy.

Given these findings, we selected ADCH charges for training ReaxFF charge parameters. Developed by Lu's group, the ADCH method, implemented in the MultiWFN package, stands out for its balance of accuracy, dependency on basis set, and efficiency in calculating dipole moments and electrostatic potentials. Notably, it offers a significantly faster alternative to wave function-based calculations.

The foundation for our C/H/O element parameters was derived from Goddard III and van Duin's pioneer work on hydrocarbon combustion. ¹⁶ We utilized the GARFfield frame-

work, which employs a genetic algorithm for the optimization of FF parameters. ⁶² This global optimization method is particularly effective for the multiparameter nonlinear optimization characteristic of FF, proving more efficient than the traditional sequential quadratic minimization method.

We initiated our FF optimization with determining the charge parameters, including shielding (EEM type), electronegativity, and hardness for the C/H/O elements. We carried out the charge calculations using our ReaxFF $_{\mathrm{CHO}}$ -S22 model and the ReaxFF models developed in 20089 (dubbed ReaxFF-08 hereafter) and 2016¹⁶ (dubbed ReaxFF-16 hereafter) with benchmark of DFT/M06-2X calculations. After optimizing 10,077 atoms, we employed the averaged Root Mean Square Error ((RMSE)) metric to assess the FF accuracy. The comparisons indicate an (RMSE) of 0.02 for our ReaxFF_{CHO}-S22 model, noticeably better than 0.03 of ReaxFF-08 and 0.05 of ReaxFF-16 models (Table 1). Subsequent validation using the Qeq module in LAMMPS for molecules both within (e.g., CH₄, C_2H_4 , and C_2H_5OH) and outside (e.g., $C_4H_{10}O$) our training set showed ReaxFF_{CHO}-S22 charge models replicated QM-derived charges more closely than ReaxFF-08 and ReaxFF-16 models, as detailed in the Supporting Information (Tables S1-S4).

3.2.2. Optimization of the Energy Parameters. To optimize further the energy parameters of the ReaxFF force field, we first fixed the optimized charge parameters discussed above. Then,

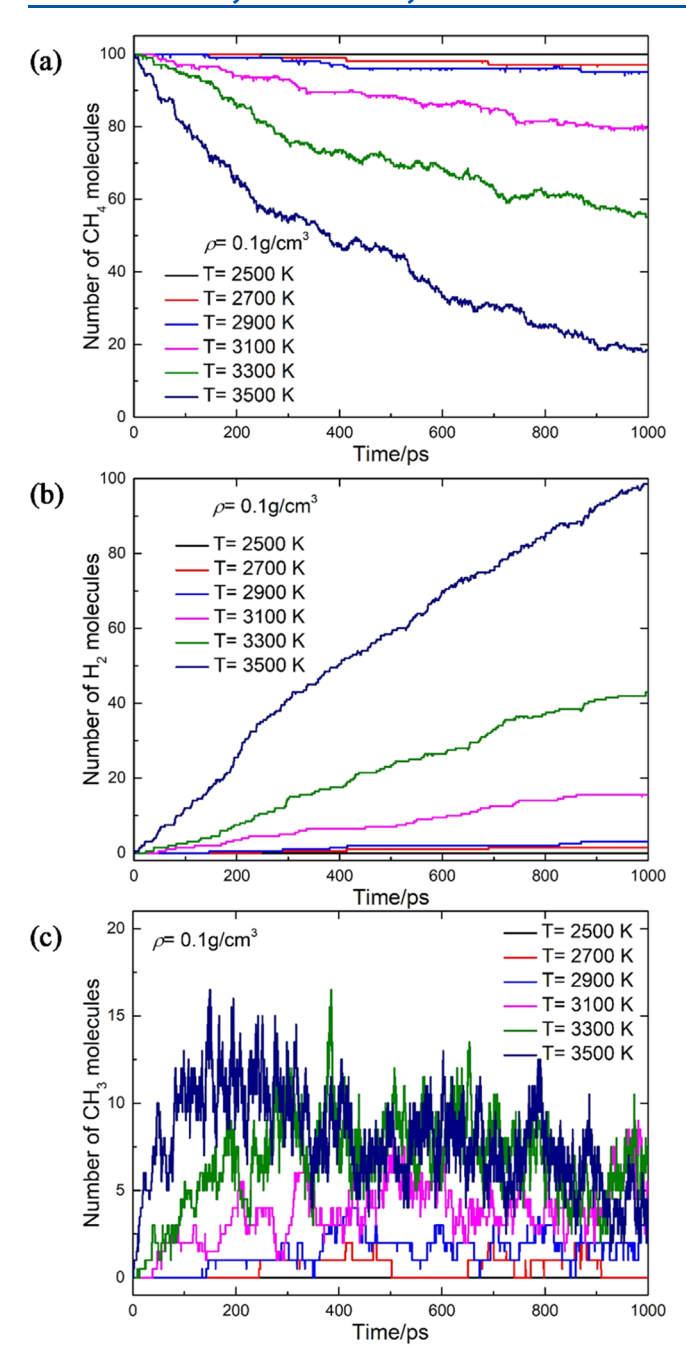


Figure 6. Number of molecules in the NVT-MD simulations at 2500 to 3500 K as functions of time: (a) reactant methane molecules; (b) product hydrogen molecules; (c) intermediate CH_3 radicals.

we segmented our QM data into two sets: one for training and another for testing. Our selection process for the training set focused on structures that represent the typical reaction scenarios of pyrolysis and combustion processes, encompassing geometries, bond dissociation energies, valence-angle distortions, torsion distortions, transition states, and reactions for various molecular geometries. The groups C0–C4 consisting of 46 small molecules were selected to cover the typical types of hydrocarbon molecules in the training data set. The larger molecules would decompose into small molecules via C–C bond cleavage during the high-temperature combustion process, so the small molecules were used to train the force field parameters, which would be more likely transferable to the cases

of large molecules. It is essential to optimize atom, off-diagonal, bond, angle, and torsion angle parameters simultaneously due to their interdependence in the final stage.

3.2.2.1. Bond Dissociation Energy Calculations. For bond dissociation energy calculations, we fixed the positions of the two atoms forming the bond of interest and optimized the coordinates of the remaining atoms. We carried out constraint geometry optimizations using the newly optimized ReaxFF_{CHO}-S22, the previous ReaxFF-08 and ReaxFF-16 models, as well as DFT/M06-2X calculations. The obtained dissociation profiles are illustrated in Figure 2 for C-H bonds in methane and C-O bonds in methanol, with additional profiles available in Figure S4. Figure 2 demonstrates that the bond length and dissociation energy trends of ReaxFF_{CHO}-S22 (red line) align more closely with the QM data (black line), showing improvements over the ReaxFF-08 (blue line) and ReaxFF-16 models (pink line). The C-H bond breakage and C-O bond formation reactions are competing key reactions critical to combustion, corresponding to reactant decomposition and product generation, respectively.

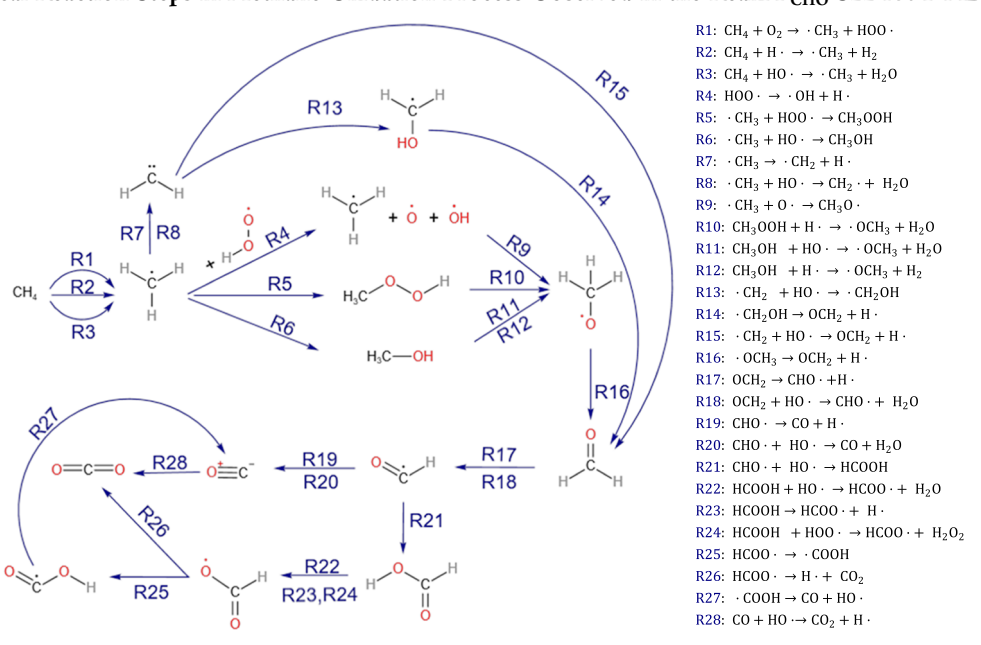
3.2.2.2. Valence Angle and Torsion Distortion Energies. The distortion energies were computed as functions of the valence angle and torsion angle using a flexible scan approach similar to that discussed above. Figures 3 and S5 display the valence-angle distortion profiles, while Figures 4 and S6 present the torsion distortion profiles. For angle parameter optimization, we calculated angle distortion energies for typical C/H/O angles, such as the C-C-C angle in propane, the C=C-C angle in propylene, the C-C-H angle in ethane, and the C= C-H angle in ethylene (Figure 3(a)-(d)). Torsion parameter optimization involved calculating torsion distortion energies for relevant C/H/O torsion angles, including the C-C-C-C torsion angle in n-butane, the H-C-O-H torsion angle in methanol, the O-C=C-H torsion angle in ethenol, and the O-O-C-C torsion angle in ethylene glycol, as depicted in Figure 4(a)-(d).

3.2.2.3. Optimization Outcomes and Transferability. The final set of optimized energy parameters for the ReaxFF force field, denoted as ReaxFF $_{\text{CHO}}$ -S22, is provided in the Supporting Information alongside charge parameters (Text S1). Figures 2–4 plot the potential energy surfaces fitted by the new ReaxFF $_{\text{CHO}}$ -S22 (red lines), showcasing enhanced agreement with QM data (black line) compared to the previous ReaxFF-08 (blue line) and ReaxFF-16 models (pink line). The $\langle \text{RMSE} \rangle$ for the training set energy is a relatively low 17.89 kcal/mol, indicating 9.3 and 15.9% improved accuracy over previous ReaxFF-08 model (19.73 kcal/mol) and ReaxFF-16 model (21.27 kcal/mol), respectively.

To assess the transferability of the ReaxFF $_{\rm CHO}$ -S22 force field, we applied it to a testing set grouped by the number of carbon atoms (C5, C6, C7, C8), revealing lower $\langle {\rm RMSE} \rangle$ values for energy calculations compared to previous ReaxFF-08 and ReaxFF-16 models across the various untrained large molecule groups (Table 2). This improvement in the validation testing sets suggests enhanced predictive capabilities of the ReaxFF $_{\rm CHO}$ -S22 model for large hydrocarbon molecules.

The examples of the validation energy curves in the test set, depicted in Figure 5(a)-(d), include calculations for the C–C bond in 2-methylbutane and the C=C bond in 2-methylbutene as well as the C–C=C angle in 2-pentene and the C–C–H angle in 2,3-dimethylpentane. These validation results for the untrained large hydrocarbon molecules indicate that the ReaxFF_{CHO}-S22 model more accurately reproduces QM findings compared to the previous ReaxFF-08 and ReaxFF-16

Scheme 1. Chemical Reaction Steps in Methane Oxidation Process Observed in the ReaxFF_{CHO}-S22 NVT-MD Simulation



models, underscoring its effectiveness and transferability in simulating chemical interactions across a wide range of hydrocarbon molecules.

3.3. Molecular Dynamics Simulations. To complement the precise results obtained from static calculations, we further conducted MD simulations. These MD simulations aimed to replicate the behavior of various chemical reactions related to the pyrolysis and combustion processes of hydrocarbon fuel, thereby validating the accuracy and applicability of our newly developed force field.

3.3.1. Molecular Dynamics Simulations of Methane Pyrolysis. Hydrocarbons, such as methane—the simplest form of an organic molecule, undergo decomposition when exposed to high temperatures. To simulate this process, we placed 100 CH₄ molecules within a simulation box at a density of 0.10 g/cm³. Following the initial energy minimization of the system, we gradually increased the temperature from 0 K to specific target temperatures (ranging from 2500 to 3500 K) using the NVT (constant number of particles, volume, and temperature) ensemble, maintaining each temperature for a duration of 1 ns (ns). Temperature control during the simulation was achieved using a Nosé—Hoover thermostat, set with a damping constant of 100 fs. The time step of 0.1 fs was used for the integration of equation of motion following Newton's second law.

Figure 6 illustrates how the rate of methane's thermal decomposition is influenced by temperature. The thermal decomposition is evidenced by the decreased number of species in CH₄ molecules and the corresponding increase in the number of H₂ molecules over time. Notably, the thermal decomposition of methane molecules occurred more often with increasing temperature. A critical reaction step in the pyrolysis is the formation of H₂ molecules, either through direct collisions between a H atom and a methane molecule or via the combination of two free H atoms. This process, resulting in an increase in both H₂ and CH₃ radical counts, shows a direct correlation with the reduction in CH₄ molecules, particularly evident in the early stages of the pyrolysis. The number of key radical CH₃ increased first due to the H abstraction of CH₄, then

decreased caused by further dehydrogenation and formation of C clusters.

3.3.2. Molecular Dynamics Simulations of Methane Oxidation. Understanding methane oxidation is a crucial fundamental step to unraveling the detailed mechanisms underlying more complex fuel combustion. To explore this process, we simulated the oxidation of methane by introducing 60 methane and 120 oxygen molecules into a periodic box measuring 34.2 × 34.2 × 34.2 ų, achieving a mass density of 0.20 g/cm³. Temperature regulation was achieved using a Nosé-Hoover thermostat, with an integration time step of 0.1 fs. The MD simulations were carried out using the Forcite program with Dreiding force field⁶³ of the Materials Studio software suite.⁶⁴ We conducted 10 independent NVT-MD simulations using the Amorphous Cell Module to generate the initial configurations. Following energy minimization of each box, we increased the temperature from 0 to 3500 K under the NVT ensemble and maintained the systems at 3500 K for 1 ns using LAMMPS imported with the newly developed ReaxFF_{CHO}-S22 parameters.

The comprehensive reaction network resulting from methane oxidation is captured in Scheme 1. This scheme highlights the initial stages of methane and oxygen combustion, beginning with the abstraction of H atoms to form 'CH3 and HOO radicals (reaction R1 in Scheme 1). Throughout the simulations, additional radicals such as ·OH and H· further contributed to the formation of ·CH3 radicals by abstracting H from CH4 molecules (R2, R3). At elevated temperatures, the O-O bond within HOO· radicals breaks, yielding ·O and ·OH radicals. Subsequently, ·O radicals combine with ·CH₃ radicals to form CH₃O· radicals (R9). Interactions between ·CH₃ and HOO· radicals result in the formation of CH₃OOH (R5), which can also produce CH₃O· radicals (R10). A significant number of · CH₃ radicals react with ·OH radicals, leading to the synthesis of methanol molecules (R6). These methanol molecules can further react with ·OH and H radicals to generate additional CH₃O· radicals (R11, R12). The high kinetic energy present at 3500 K facilitates the breaking of the C-H bond in ·CH₃ radicals, producing H₂C: radicals that can then form ·CH₂OH

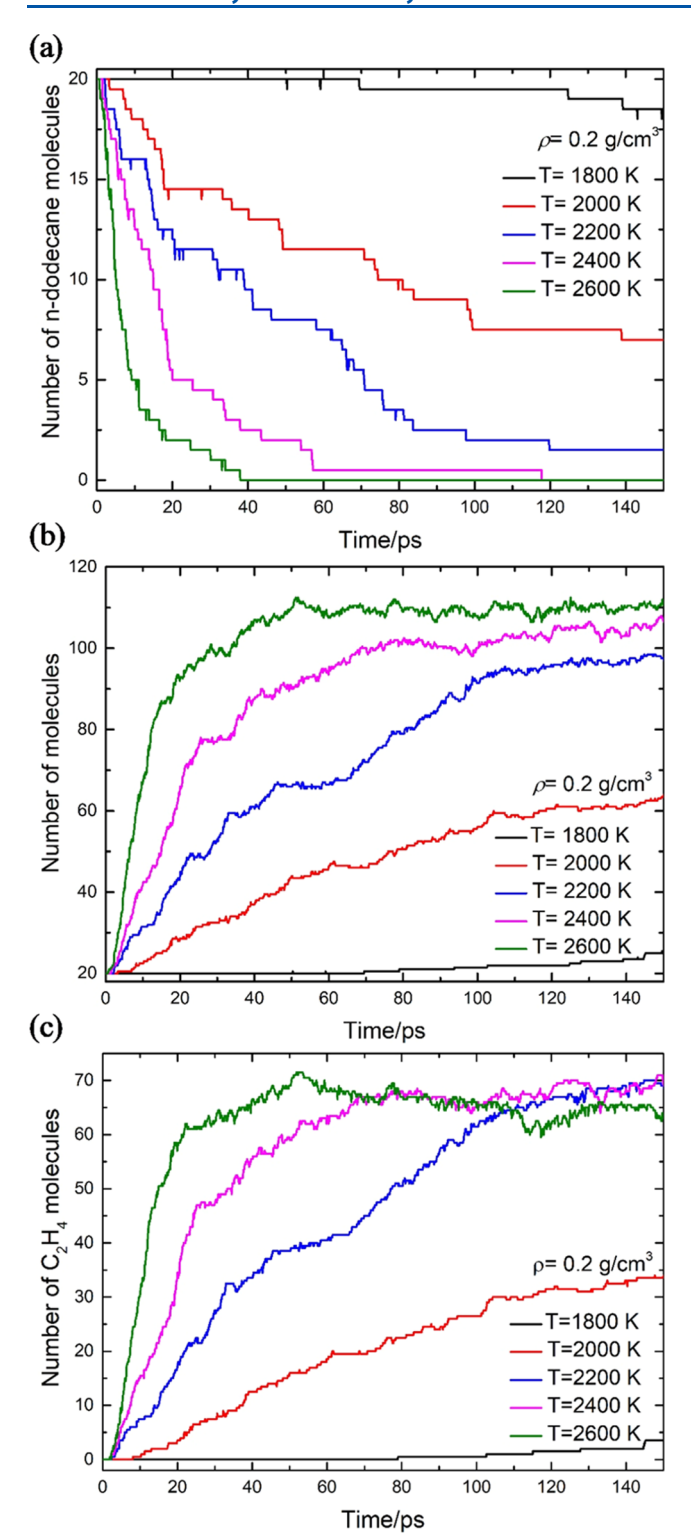


Figure 7. Number of molecules in the NVT-MD simulations as functions of time at 1800-2600 K: (a) the number of n-dodecane molecules; (b) total population of all molecules; and (c) the number of ethylene molecules.

radicals (R13). The C–H bond within ·CH₂OH radicals also breaks, resulting in the formation of formaldehyde (CH₂O, R14, R15, and R16).

The transformation of CH_2O molecules into formyl (·CHO) radicals (R17 and R18) marks another critical pathway, where formyl radicals can either lose a H radical to become CO or react

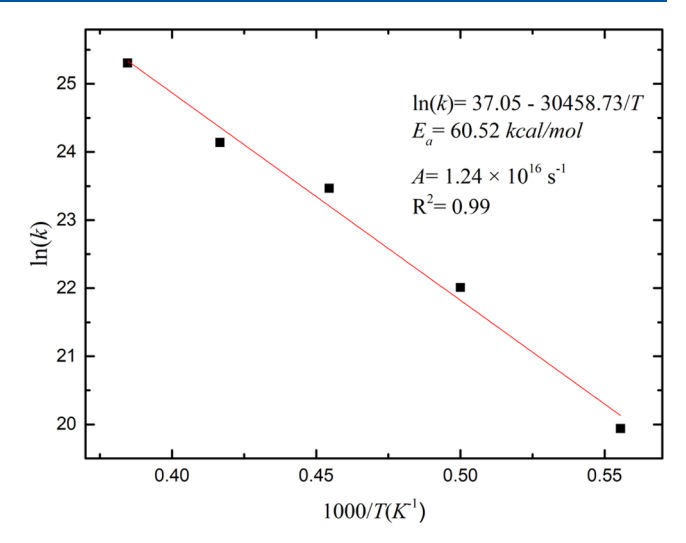


Figure 8. Reaction rate constant, $\ln(k)$, as functions of temperature T obtained from the ReaxFF_{CHO}-S22 NVT-MD simulations of n-dodecane molecules. Inset is the Arrhenius equation with fitted parameters including activation energy $E_{\rm a}$ and prefactor A.

with ·OH radicals (R19, R20). Additionally, formyl radicals can interact with ·OH radicals to produce formic acid (HCOOH, R21), subsequently generating ·OOCH radicals (R21, R22, R23). These ·OOCH radicals can then convert to $\rm CO_2$ (R26) and ·COOH radicals (R25), with the latter further transforming into CO (R27). Moreover, OH radicals can react with CO molecules to yield $\rm CO_2$ and H· radicals (R28), showcasing a series of reactions consistent with previously established major reaction paths. 32,65,66

3.3.3. Molecular Dynamics Simulations of n-Dodecane Decomposition. This study examines how temperature influences the pyrolysis of n-dodecane, a large hydrocarbon molecule, employing a series of NVT-MD simulations across a range from 1800 to 2600 K, with 200 K intervals, over a total simulation duration of 150 ps. We placed 20 n-dodecane molecules in a simulation box with a mass density of 0.20 g/cm^3 . Figure 7 captures the dynamic changes in the number of ndodecane molecules, total molecules, and ethylene molecules over time. Notably, n-dodecane decomposition initiates at 69.4 ps at 1800 K, with the onset occurring within 10 ps at higher temperatures. As the simulation temperature increases, both the total number of fragments and the consumption rate of ndodecane rise. Ethylene consistently emerges as the most prevalent molecule in all simulations, in agreement with experimental findings.⁶⁷ At the highest temperature of 2600 K, the quantity of ethylene molecules stabilizes, fluctuating around a constant value after approximately 40 ps, indicating the complete decomposition of *n*-dodecane molecules by this point.

The decomposition process adheres to the kinetic model of first-order reactions, described by the formula:

$$ln N - ln N_0 = kt$$
(2)

In this equation, the concentration of n-dodecane is represented by the number of molecules where N_0 and N denote the initial and current numbers of molecules respectively, k is the reaction rate constant, and t is the time elapsed. Based on the data presented in Figure 7a, we derived k as a function of the temperature. The Arrhenius equation, which describes the relationship between the reaction rate constant (k) and temperature (T), is given as

$$\ln(k) = -\frac{E_a}{R} \frac{1}{T} + \ln(A) \tag{3}$$

Here, $E_{\rm a}$ represents the reaction's activation energy, A is the pre-exponential factor, and R is the universal gas constant (8.31446261815324 J·K⁻¹·mol⁻¹). Figure 8 shows the fitting results, yielding $E_{\rm a}=60.52$ kcal/mol and $A=1.24\times10^{16}$ s⁻¹, closely matching experimental data ($E_{\rm a}=60.00$ kcal/mol, $A=1.06\times10^{16}$ s⁻¹). The excellent agreement among our simulation-derived decomposition pathways, Arrhenius parameters, and experimental observations underscores the applicability of the ReaxFF_{CHO}-S22 force field across different hydrocarbon sizes, from small to large molecules.

4. CONCLUSIONS AND PERSPECTIVE

This research has successfully developed an accurate and transferable ReaxFF_{CHO}-S22 reactive force field, specifically tailored for carbon, hydrogen, and oxygen (C/H/O) systems. This advancement was achieved through more accurate benchmark data sets generated by high-level QM calculations with the meta-GGA DFT functional M06-2X including a large basis set and a consistent charge scheme, with a more diverse polymorphous training set from small to large hydrocarbon molecules, along with the meticulous global optimization of multiple interrelated parameters, allowing for an accurate representation of both training and testing data sets. Compared with its predecessors, ReaxFF_{CHO}-S22 exhibits statistically lower RMSE in static calculations for a large variety of hydrocarbon molecules, highlighting its superior transferability and universality across various C/H/O systems.

Employing ReaxFF_{CHO}-S22, we conducted prototypical molecular dynamics simulations to examine the pyrolysis of methane, the oxidation of methane, and the pyrolysis of *n*-dodecane. These simulation results confirm that ReaxFF_{CHO}-S22 is adept at capturing the complex dynamics of hydrocarbon reactions. These capabilities underscore the potential of the ReaxFF_{CHO}-S22 force field as a powerful tool for computational research, offering new insights into the atomic-level mechanisms of reactions pertinent to hydrocarbon fuels, biofuels, and energetic materials. Note that ReaxFF_{CHO}-S22 is mainly developed for combustion of hydrocarbon molecules, and the suitability of its applications on the bulk carbon materials needs to be validated with caution.

This work sets a new benchmark for future studies aiming to unravel the complexities of chemical reaction mechanisms and dynamics within these critical domains at the molecular level. This foundational work not only enhances our understanding of complex chemical systems but also sets a precedent for future computational chemistry endeavors, driving forward the capabilities of molecular dynamics simulations to capture the essence of chemical reactivity and interactions. The data-based machine learning potentials (MLPs)^{68–70} are emerging recently to show the capabilities of describing bond breaking and formation. It would be interesting to compare the performance of the analytical ReaxFF potentials with the data-based MLPs in the future.

The transferability and comprehensive applicability of ReaxFF across a wide range of materials and reactions have made it a cornerstone tool in computational chemistry and materials science. Its continued development and refinement promise to further expand its application potential, providing deeper insights into the atomistic details of the chemical reactions and material properties. The application of ReaxFF to

study the pyrolysis and combustion of hydrocarbon fuels exemplifies its strength in tackling complex chemical processes, contributing to our understanding of these fundamental reactions with implications for energy production, environmental science, and beyond.

ASSOCIATED CONTENT

Supporting Information

The Supporting Information is available free of charge at https://pubs.acs.org/doi/10.1021/acs.jpca.4c01924.

Averaged absolute errors of QEq charges in ReaxFF_{CHO}S22 relative to QM charges for CH₄, C₂H₄, C₂H₅OH, and C₄H₁₀O molecules; valence bond dissociation energy, valence-angle distortion energy, and torsion angle distortion energy as functions of distances for various hydrocarbon molecules as well as key reaction energies related to hydrocarbon combustions calculated using ReaxFF_{CHO}-S22, ReaxFF_{CHO}-08, ReaxFF_{CHO}-16, and QM (6-311++G**/M06-2X); ReaxFF_{CHO}-S22 force field parameters. (PDF)

AUTHOR INFORMATION

Corresponding Author

Yi Liu — Materials Genome Institute, Shanghai Engineering Research Center for Integrated Circuits and Advanced Display Materials, Shanghai University, Shanghai 200444, China; Materials and Process Simulation Center (MSC), California Institute of Technology, Pasadena, California 91125, United States; orcid.org/0000-0002-5821-9086; Email: yiliu@shu.edu.cn

Authors

Qingqing Wang — Materials Genome Institute, Shanghai Engineering Research Center for Integrated Circuits and Advanced Display Materials, Shanghai University, Shanghai 200444, China

Qi He — Materials Genome Institute, Shanghai Engineering Research Center for Integrated Circuits and Advanced Display Materials, Shanghai University, Shanghai 200444, China

Bin Xiao – Materials Genome Institute, Shanghai Engineering Research Center for Integrated Circuits and Advanced Display Materials, Shanghai University, Shanghai 200444, China

Dong Zhai — Materials Genome Institute, Shanghai Engineering Research Center for Integrated Circuits and Advanced Display Materials, Shanghai University, Shanghai 200444, China; orcid.org/0000-0003-3155-4607

Yiheng Shen — Materials Genome Institute, Shanghai Engineering Research Center for Integrated Circuits and Advanced Display Materials, Shanghai University, Shanghai 200444, China

William A. Goddard, III – Materials and Process Simulation Center (MSC), California Institute of Technology, Pasadena, California 91125, United States; orcid.org/0000-0003-0097-5716

Complete contact information is available at: https://pubs.acs.org/10.1021/acs.jpca.4c01924

Author Contributions

Q.W.: Investigation, formal analysis, visualization, writing—original draft. Q.H.: Resources—provision of study materials. B.X.: Resources—provision of study materials. D.Z.: Resources—provision of study materials. Y.S.: Writing—review and

editing. Y.L.: Conceptualization, supervision, formal analysis, writing—review and editing. W.A.G. III: Review and editing.

Notes

The authors declare no competing financial interest.

ACKNOWLEDGMENTS

We thank the financial supports of the National Natural Science Foundation of China (Nos. 52373227 and 91641128) and National Key R&D Program of China (Nos. 2017YFB0701502 and 2017YFB0702901). W.A.G. III acknowledges support from the US National Science Foundation (CBET 2311117). This work was also supported by the Shanghai Technical Service Center for Advanced Ceramics Structure Design and Precision Manufacturing (No. 20DZ2294000) and Shanghai Technical Service Center of Science and Engineering Computing, Shanghai University. The authors acknowledge the Beijing Super Cloud Computing Center, Hefei Advanced Computing Center, and Shanghai University for providing HPC resources.

REFERENCES

- (1) Tran, L. S.; Sirjean, B.; Glaude, P.-A.; Fournet, R.; Battin-Leclerc, F. Progress in detailed kinetic modeling of the combustion of oxygenated components of biofuels. *Energy* **2012**, 43 (1), 4–18.
- (2) Sarathy, S. M.; Oßwald, P.; Hansen, N.; Kohse-Höinghaus, K. Alcohol combustion chemistry. *Prog. Energy Combust. Sci.* **2014**, *44*, 40–102.
- (3) Zheng, J.; Truhlar, D. G. Quantum Thermochemistry: Multi-structural Method with Torsional Anharmonicity Based on a Coupled Torsional Potential. *J. Chem. Theory Comput.* **2013**, *9* (3), 1356–1367.
- (4) Qi, F.; Li, Y.; Zeng, M.; Zhang, F. Progress and perspectives in combustion chemistry. *J. Univ. Sci. Technol. China* **2013**, 43 (11), 948–958.
- (5) Jasper, A. W.; Pelzer, K. M.; Miller, J. A.; Kamarchik, E.; Harding, L. B.; Klippenstein, S. J. Predictive a priori pressure-dependent kinetics. *Science* **2014**, *346*, 1212–1215.
- (6) van Duin, A. C. T.; Dasgupta, S.; Lorant, F.; Goddard, W. A., III ReaxFF: A Reactive Force Field for Hydrocarbons. *J. Phys. Chem. A* **2001**, *105* (41), 9396–9409, DOI: 10.1021/jp004368u.
- (7) Mortier, W. J.; Ghosh, S. K.; Shankar, S. Electronegativity-equalization method for the calculation of atomic charges in molecules. *J. Am. Chem. Soc.* **1986**, *108* (15), 4315–4320.
- (8) Rappe, A. K.; Goddard, W. A. Charge equilibration for molecular dynamics simulations. *J. Phys. Chem. A* **1991**, *95* (8), 3358–3363.
- (9) Chenoweth, K.; van Duin, A. C. T.; Goddard, W. A. ReaxFF Reactive Force Field for Molecular Dynamics Simulations of Hydrocarbon Oxidation. *J. Phys. Chem. A* **2008**, *112* (5), 1040–1053.
- (10) Chenoweth, K.; van Duin, A. C. T.; Dasgupta, S.; Goddard, W. A., III Initiation Mechanisms and Kinetics of Pyrolysis and Combustion of JP-10 Hydrocarbon Jet Fuel. *J. Phys. Chem. A* **2009**, *113* (9), 1740–1746, DOI: 10.1021/jp8081479.
- (11) Page, A. J.; Moghtaderi, B. Molecular Dynamics Simulation of the Low-Temperature Partial Oxidation of CH₄. *J. Phys. Chem. A* **2009**, *113* (8), 1539–1547.
- (12) Kamat, A. M.; van Duin, A. C. T.; Yakovlev, A. Molecular Dynamics Simulations of Laser-Induced Incandescence of Soot Using an Extended ReaxFF Reactive Force Field. *J. Phys. Chem. A* **2010**, *114* (48), 12561–12572.
- (13) Mueller, J. E.; van Duin, A. C. T.; Goddard, W. A. Application of the ReaxFF Reactive Force Field to Reactive Dynamics of Hydrocarbon Chemisorption and Decomposition. *J. Phys. Chem. C* **2010**, *114* (12), 5675–5685.
- (14) Liu, L.; Bai, C.; Sun, H.; Goddard, W. A. Mechanism and Kinetics for the Initial Steps of Pyrolysis and Combustion of 1,6-Dicyclopropane-2,4-hexyne from ReaxFF Reactive Dynamics. *J. Phys. Chem. A* **2011**, *115* (19), 4941–4950.
- (15) Wang, Q.-D.; Wang, J.-B.; Li, J.-Q.; Tan, N.-X.; Li, X.-Y. Reactive molecular dynamics simulation and chemical kinetic modeling of

- pyrolysis and combustion of n-dodecane. Combust. Flame 2011, 158 (2), 217-226.
- (16) Ashraf, C.; van Duin, A. C. Extension of the ReaxFF Combustion Force Field toward Syngas Combustion and Initial Oxidation Kinetics. *J. Phys. Chem. A* **2017**, *121* (5), 1051–1068.
- (17) Li, X.; Zheng, M.; Ren, C.; Guo, L. ReaxFF Molecular Dynamics Simulations of Thermal Reactivity of Various Fuels in Pyrolysis and Combustion. *Energy Fuels* **2021**, *35* (15), 11707–11739.
- (18) Budzien, J.; Thompson, A. P.; Zybin, S. V. Reactive Molecular Dynamics Simulations of Shock Through a Single Crystal of Pentaerythritol Tetranitrate. *J. Phys. Chem. B* **2009**, *113* (40), 13142–13151.
- (19) Zhang, L.; Zybin, S. V.; van Duin, A. C. T.; Dasgupta, S.; Goddard, W. A.; Kober, E. M. Carbon Cluster Formation during Thermal Decomposition of Octahydro-1,3,5,7-tetranitro-1,3,5,7-tetrazocine and 1,3,5-Triamino-2,4,6-trinitrobenzene High Explosives from ReaxFF Reactive Molecular Dynamics Simulations. *J. Phys. Chem. A* **2009**, *113* (40), 10619–10640.
- (20) Zhang, L.; Zybin, S. V.; Van Duin, A. C. T.; Goddard, W. A. Modeling High Rate Impact Sensitivity of Perfect RDX and HMX Crystals by ReaxFF Reactive Dynamics. *J. Energ. Mater.* **2010**, 28, 92–127.
- (21) An, Q.; Liu, Y.; Zybin, S. V.; Kim, H.; Goddard, W. A. Anisotropic Shock Sensitivity of Cyclotrimethylene Trinitramine (RDX) from Compress-and-Shear Reactive Dynamics. *J. Phys. Chem. C* **2012**, *116* (18), 10198–10206.
- (22) Furman, D.; Kosloff, R.; Dubnikova, F.; Zybin, S. V.; Goddard, W. A.; Rom, N.; Hirshberg, B.; Zeiri, Y. Decomposition of Condensed Phase Energetic Materials: Interplay between Uni- and Bimolecular Mechanisms. *J. Am. Chem. Soc.* **2014**, *136* (11), 4192–4200.
- (23) Shan, T.-R.; van Duin, A. C. T.; Thompson, A. P. Development of a ReaxFF Reactive Force Field for Ammonium Nitrate and Application to Shock Compression and Thermal Decomposition. *J. Phys. Chem. A* **2014**, *118* (8), 1469–1478.
- (24) Zhou, T.; Song, H.; Liu, Y.; Huang, F. Shock initiated thermal and chemical responses of HMX crystal from ReaxFF molecular dynamics simulation. *Phys. Chem. Chem. Phys.* **2014**, *16* (27), 13914–13931
- (25) Liu, Y.; Zybin, S. V.; Guo, J.; van Duin, A. C. T.; Goddard, W. A., III Reactive Dynamics Study of Hypergolic Bipropellants: Monomethylhydrazine and Dinitrogen Tetroxide. *J. Phys. Chem. B* **2012**, *116* (48), 14136–14145.
- (26) Chenoweth, K.; Cheung, S.; van Duin, A. C. T.; Goddard, W. A.; Kober, E. M. Simulations on the Thermal Decomposition of a Poly(dimethylsiloxane) Polymer Using the ReaxFF Reactive Force Field. J. Am. Chem. Soc. 2005, 127 (19), 7192–7202.
- (27) Zhang, J.; Weng, X.; Han, Y.; Li, W.; Cheng, J.; Gan, Z.; Gu, J. The effect of supercritical water on coal pyrolysis and hydrogen production: A combined ReaxFF and DFT study. *Fuel* **2013**, *108*, 682–690.
- (28) Zheng, M.; Li, X.; Liu, J.; Guo, L. Initial Chemical Reaction Simulation of Coal Pyrolysis via ReaxFF Molecular Dynamics. *Energy Fuels* **2013**, 27 (6), 2942–2951.
- (29) Zheng, M.; Li, X.; Liu, J.; Wang, Z.; Gong, X.; Guo, L.; Song, W. Pyrolysis of Liulin Coal Simulated by GPU-Based ReaxFF MD with Cheminformatics Analysis. *Energy Fuels* **2014**, *28* (1), 522–534.
- (30) Bhoi, S.; Banerjee, T.; Mohanty, K. Molecular dynamic simulation of spontaneous combustion and pyrolysis of brown coal using ReaxFF. *Fuel* **2014**, *136*, 326–333.
- (31) Wang, H.; Feng, Y.; Zhang, X.; Lin, W.; Zhao, Y. Study of coal hydropyrolysis and desulfurization by ReaxFF molecular dynamics simulation. *Fuel* **2015**, *145*, 241–248.
- (32) Liang, Y.-H.; Wang, F.; Zhang, H.; Wang, J.-P.; Li, Y.-Y.; Li, G.-Y. A ReaxFF molecular dynamics study on the mechanism of organic sulfur transformation in the hydropyrolysis process of lignite. *Fuel Process. Technol.* **2016**, *147*, 32–40.
- (33) Zhang, T.; Li, X.; Qiao, X.; Zheng, M.; Guo, L.; Song, W.; Lin, W. Initial Mechanisms for an Overall Behavior of Lignin Pyrolysis through

- Large-Scale ReaxFF Molecular Dynamics Simulations. *Energy Fuels* **2016**, 30 (4), 3140–3150.
- (34) Hong, D.; Liu, L.; Zhang, S.; Guo, X. Effect of cooling rate on the reaction of volatiles from low-rank coal pyrolysis: Molecular dynamics simulations using ReaxFF. Fuel Process. Technol. **2018**, 178, 133–138.
- (35) Hong, D.; Li, P.; Si, T.; Guo, X. ReaxFF simulations of the synergistic effect mechanisms during co-pyrolysis of coal and polyethylene/polystyrene. *Energy* **2021**, *218*, No. 119553.
- (36) Ojwang', J. G. O.; van Santen, R.; Kramer, G. J.; van Duin, A. C.; Goddard, W. A., III Predictions of melting, crystallization, and local atomic arrangements of aluminum clusters using a reactive force field. *J. Chem. Phys.* **2008**, *129* (24), No. 244506.
- (37) Han, S. S.; Choi, S. H.; van Duin, A. C. Molecular dynamics simulations of stability of metal-organic frameworks against H2O using the ReaxFF reactive force field. *Chem. Commun.* **2010**, 46 (31), 5713–5715.
- (38) Senftle, T. P.; Meyer, R. J.; Janik, M. J.; van Duin, A. C. Development of a ReaxFF potential for PdO and application to palladium oxide formation. *J. Chem. Phys.* **2013**, *139* (4), No. 044109.
- (39) Stephens, P. J.; Devlin, F. J.; Chabalowski, C. F.; Frisch, M. J. Ab Initio Calculation of Vibrational Absorption and Circular Dichroism Spectra Using Density Functional Force Fields. *J. Phys. Chem. A* **1994**, 98, 11623–11627.
- (40) Hehre, W. J.; Random, L.; Schleyer, P. v. R.; Pople, J. A.; Wiley, J. Ab Initio Molecular Orbital Theory; Wiley: New York, 1986.
- (41) Lu, T.; Chen, F. Atomic Dipole Moment Corrected Hirshfeld Population Method. J. Theor. Comput. Chem. 2012, 11 (01), 163–183.
- (42) Holland, J. H. Adaptation in Natural and Artificial Systems: An Introductory Analysis with Applications to Biology, Control, and Artificial Intelligence; MIT Press: Cambridge, MA, 1992.
- (43) Frisch, M. J.; Schlegel, H. B.; Scuseria, G. E.; Robb, M. A.; Cheeseman, J. R.; Scalmani, G.; Barone, V.; Mennucci, B.; Petersson, G. A.; Nakatsuji, H.; Caricato, M.; Li, X.; Hratchian, H. P.; Izmaylov, A. F.; Bloino, J.; Zheng, G.; Sonnenberg, J. L.; Hada, M.; Ehara, M.; Toyota, K.; Fukuda, R.; Hasegawa, J.; Ishida, M.; Nakajima, T.; Honda, Y.; Kitao, O.; Nakai, H.; Vreven, T.; Montgomery, J. A., Jr.; Peralta, J. E.; Ogliaro, F.; Bearpark, M.; Heyd, J. J.; Brothers, E.; Kudin, K. N.; Staroverov, V. N.; Keith, T.; Kobayashi, R.; Normand, J.; Raghavachari, K.; Rendell, A.; Burant, J. C.; Iyengar, S. S.; Tomasi, J.; Cossi, M.; Rega, N.; Millam, J. M.; Klene, M.; Knox, J. E.; Cross, J. B.; Bakken, V.; Adamo, C.; Jaramillo, J.; Gomperts, R.; Stratmann, R. E.; Yazyev, O.; Austin, A. J.; Cammi, R.; Pomelli, C.; Ochterski, J. W.; Martin, R. L.; Morokuma, K.; Zakrzewski, V. G.; Voth, G. A.; Salvador, P.; Dannenberg, J. J.; Dapprich, S.; Daniels, A. D.; Farkas, O.; Foresman, J. B.; Ortiz, J. V.; Cioslowski, J.; Fox, D. J. Gaussian 09, Revision D.01; Gaussian Inc.: Wallingford, CT, 2009.
- (44) Zhao, Y.; Truhlar, D. G. The M06 suite of density functionals for main group thermochemistry, thermochemical kinetics, noncovalent interactions, excited states, and transition elements: two new functionals and systematic testing of four M06-class functionals and 12 other functionals. *Theor. Chem. Acc.* 2008, 120 (1–3), 215–241.
- (45) Plimpton, S. J. Fast Parallel Algorithms for Short-Range Molecular Dynamics. *J. Comput. Phys.* **1995**, *117*, 1–19.
- (46) Aktulga, H. M.; Fogarty, J. C.; Pandit, S. A.; Grama, A. Y. Parallel reactive molecular dynamics: Numerical methods and algorithmic techniques. *Parallel Comput.* **2012**, 38 (4–5), 245–259.
- (47) Liu, J.; Li, X.; Guo, L.; Zheng, M.; Han, J.; Yuan, X.; Nie, F.; Liu, X. Reaction analysis and visualization of ReaxFF molecular dynamics simulations. *J. Mol. Graphics Model.* **2014**, *53*, 13–22.
- (48) Han, J.; Li, X.; Guo, L.; Zheng, M.; Qiao, X.; Liu, X.; Mingjie; Gao; Zhang, T.; Han, S. Automatic classification and visualization of species and reactions obtained from ReaxFF MD simulations. *Comput. Appl. Chem.* **2015**, 32 (05), 519–526.
- (49) Tang, Y.; Zheng, M.; Ren, C.; Li, X.; Guo, L. Visualized Reaction Tracking and Physical Property Analysis for a Picked 3D Area in a Reactive Molecular Dynamics Simulation System. *Acta Phys.—Chim. Sin.* **2021**, 37 (10), 77—87.

- (50) Gao, C. W.; Allen, J. W.; Green, W. H.; West, R. H. Reaction Mechanism Generator: Automatic construction of chemical kinetic mechanisms. *Comput. Phys. Commun.* **2016**, 203, 212–225.
- (51) Mulliken, R. S. Electronic Population Analysis on LCAO-MO Molecular Wave Functions. I. J. Chem. Phys. 1955, 23 (10), 1833–1840.
- (52) Mulliken, R. S. Electronic Population Analysis on LCAO–MO Molecular Wave Functions. II. Overlap Populations, Bond Orders, and Covalent Bond Energies. *J. Chem. Phys.* **1955**, 23 (10), 1841–1846.
- (53) Mulliken, R. S. Electronic Population Analysis on LCAO-MO Molecular Wave Functions. III. Effects of Hybridization on Overlap and Gross AO Populations. *J. Chem. Phys.* **1955**, 23 (12), 2338–2342.
- (54) Reed, A. E.; Weinstock, R. B.; Weinhold, F. Natural population analysis. *J. Chem. Phys.* **1985**, *83* (2), 735–746.
- (55) Momany, F. A. Determination of partial atomic charges from ab initio molecular electrostatic potentials. Application to formamide, methanol, and formic acid. *J. Phys. Chem. A* **1978**, 82 (5), 592–601.
- (56) Cox, S. R.; Williams, a. D. E. Representation of the Molecular Electrostatic Potential by a Net Atomic Charge Model. *J. Comput. Chem.* **1981**, 2 (3), 304–323.
- (57) Singh, U. C.; Kollman, a. P. A. An approach to computing electrostatic charges for molecules. *J. Comput. Chem.* **1984**, *S* (2), 129–145
- (58) Bayly, C. I.; Cieplak, P.; Cornell, W. D.; Kollman, a. P. A. A Well-Behaved Electrostatic Potential Based Method Using Charge Restraints for Deriving. *J. Phys. Chem. A* **1993**, *97*, 10269–10280.
- (59) Jakalian, A.; Bush, B. L.; Jack, D. B.; Bayly, C. I. Fast, efficient generation of high-quality atomic charges. AM1-BCC model I. Method. *J. Comput. Chem.* **2000**, *21* (2), 132–146.
- (60) Jakalian, A.; Jack, D. B.; Bayly, C. I. Fast, efficient generation of high-quality atomic charges. AM1-BCC model: II. Parameterization and validation. *J. Comput. Chem.* **2002**, 23 (16), 1623–1641.
- (61) Lu, T.; Chen, F. Multiwfn: a multifunctional wavefunction analyzer. J. Comput. Chem. 2012, 33 (5), 580-592.
- (62) Jaramillo-Botero, A.; Naserifar, S.; Goddard, W. A., 3rd. General Multiobjective Force Field Optimization Framework, with Application to Reactive Force Fields for Silicon Carbide. *J. Chem. Theory Comput* **2014**, *10* (4), 1426–1439.
- (63) Mayo, S. L.; Olafson, B. D.; Goddard, W. A. DREIDING: a generic force field for molecular simulations. *J. Phys. Chem. A* **1990**, *94* (26), 8897–8909.
- (64) Accelrys. Materials Studio 2020 https://www.3ds.com/products/biovia/materials-studio.
- (65) Reid, I. A. B.; Robinson, C. G.; Smith, D. B. Spontaneous ignition of methane: Measurement and chemical model. *Symp. (Int.) Combust.* **1985**, 20 (1), 1833–1843, DOI: 10.1016/S0082-0784(85)80681-0.
- (66) Zeng, J.; Cao, L.; Xu, M.; Zhu, T.; Zhang, J. Z. H. Complex reaction processes in combustion unraveled by neural network-based molecular dynamics simulation. *Nat. Commun.* **2020**, *11* (1), No. 5713.
- (67) MacDonald, M. E.; Ren, W.; Zhu, Y.; Davidson, D. F.; Hanson, R. K. Fuel and Ethylene Measurements during n-dodecane, methylcyclohexane, and iso-cetane pyrolysis in shock tubes. *Fuel* **2013**, *103*, 1060–1068
- (68) Rowe, P.; Deringer, V. L.; Gasparotto, P.; Csányi, G.; Michaelides, A. An accurate and transferable machine learning potential for carbon. *I. Chem. Phys.* **2020**, *153* (3), No. 034702.
- (69) Csányi, G.; Morgan, J. W. R.; Wales, D. J. Global analysis of energy landscapes for materials modeling: A test case for C60. *J. Chem. Phys.* **2023**, *159* (10), No. 104107, DOI: 10.1063/5.0167857.
- (70) Qamar, M.; Mrovec, M.; Lysogorskiy, Y.; Bochkarev, A.; Drautz, R. Atomic Cluster Expansion for Quantum-Accurate Large-Scale Simulations of Carbon. *J. Chem. Theory Comput.* **2023**, *19* (15), 5151–5167